Flow Accelerates Adhesion Between Functional Polyethylene and Polyurethane

Jie Song
Dept. of Chemical Engineering and Materials Science, University of Minnesota, Minneapolis, MN 55455

Randy H. Ewoldt
Institute for Mathematics and its Applications & Dept. of Chemical Engineering and Materials Science, University of Minnesota, Minneapolis, MN 55455

Wanli Hu
Dept. of Chemical Engineering and Materials Science, University of Minnesota, Minneapolis, MN 55455

H. Craig Silvis
Corporate Research & Development, The Dow Chemical Company, Midland, MI 48674

Christopher W. Macosko
Dept. of Chemical Engineering and Materials Science, University of Minnesota, Minneapolis, MN 55455

DOI 10.1002/aic.12551
Published online March 2, 2011 in Wiley Online Library (wileyonlinelibrary.com).

Polyethylene (PE) has relatively poor adhesion with polar polymeric materials. In an effort to improve the adhesion between PE and thermoplastic polyurethane (TPU), maleic anhydride (MA), hydroxyl (OH), and secondary amine (NHR) functionalized PEs were blended into nonmodified PE. These functional groups will react with urethane linkages in TPU at the temperature of melt processing. We bonded these PEs to TPU via lamination and coextrusion. To compare the two processes, we determined the interfacial copolymer density Σ considering both advection and interfacial area generation. We found that the development of adhesion in coextrusion was much faster in comparison with lamination at the same temperature. This difference was attributed to the extensional and compressive flow in coextrusion overcoming the diffusion barrier at the interface and forcing reactive species to penetrate the interface. The effects of functional group reactivity and processing variables on adhesion were correlated with interfacial copolymer coverage. Amine functionalized PE showed dramatic adhesion improvement even at 1 wt %. © 2011 American Institute of Chemical Engineers *AIChE J,* 57: 3496–3506, 2011

Keywords: polymer adhesion, interface, coupling reaction, flow, kinetics

Introduction

As the workhorses of the plastic industry, polyolefins are consumed in the largest volume of all types of polymers. Owing to their remarkable resistance to harsh chemical environment and a wide range of physical properties, polyolefins are found in a variety of applications including food packaging, high strength fibers, building materials, and automotive exterior parts. Despite their wide spread use, polyolefins suffer from relatively poor adhesion and compatibility with more polar polymeric materials because of their intrinsic low polarity and lack of reactive functional groups.[1–5]

Correspondence concerning this article should be addressed to C. W. Macosko at macosko@umn.edu.

Adhesion between two immiscible polymers is usually very weak because there is little entanglement across the interface.[6–8] Adhesion can be enhanced by adding a compatibilizer that is capable of staying at the interface and entangling with both sides. This kind of "stitching"[9–11] can be created by at least three methods: (1) adding premade block copolymers; (2) adding a tie layer, a third polymer which is at least partially miscible in each of the immiscible polymers; and (3) forming copolymers in situ via coupling reactions at polymer–polymer interfaces. Premade copolymers tend to embed in the bulk phases, reducing the concentration of copolymers available in interfaces. A tie layer always requires a separate layer of a third component. Interfacial coupling reactions improve adhesion by generating copolymers and "stitching" across the interface. Coupling reactions have some advantages over the other two methods: (1) most of the copolymers formed stay at the interface; (2) coupling reactions can link many homopolymer pairs for which the complementary block copolymer synthesis is not available; and (3) they also give processing simplicity as there is no need for a third layer.

Most studies of adhesion have focused on glassy or semicrystalline polymers and only a few involved elastomers.[6,7,9–11] However, in practice, there is much interest in combining the properties of elastomers through adhesion, for example, polyethylene (PE) elastomers, which have excellent extensibility, flexibility, and low cost, and thermoplastic polyurethanes (TPU), which have high elasticity, abrasion resistance, and impact strength. Using the coupling reaction strategy, adhesion to polyurethane substrates can be improved using a polyolefin with functional groups that can react with urethane linkages.[12,13] For example, Lu et al. found that adhesion between TPU and polypropylene (PP) was greatly promoted by secondary amine-functionalized PP, whereas almost no adhesion was found between TPU and PP homopolymers and only modest improvement with maleic anhydride (MA) functionalized PP.[14] Lu et al. attributed improved adhesion to coupling of the functional PP with isocyanate groups released from urethane linkages in TPU at melt processing temperature.

In this research, we grafted MA, hydroxyl (OH), and secondary amine (NHR) functional groups onto ethylene/1-octene random copolymers through a continuous reactive extrusion process. We measured the peel strength of the functional PEs bonded to TPU through lamination and coextrusion. Our goal is to understand the effects of reactivity of functional groups and processing variables on adhesion. We compare lamination and coextrusion at the same reaction time and temperature and, remarkably, we find coextrusion builds adhesion faster.

Experimental

Materials

Ethylene/1-octene random copolymer (ENGAGE^{TM}8200), LLDPE-1, was provided by The Dow Chemical Company. This copolymer has 7.3 mol % octene with a melt flow rate (MFR) of 5.0 dg/min as measured by ASTM D 1238 and density of 0.870 g/cm^3 as measured by ASTM D 792. The anhydride-functionalized ethylene/1-octene copolymer (PE-MA) was prepared by free radical grafting of MA onto another ethylene/1-octene copolymer LLDPE-2 (ENGAGE^{TM}8407) in the melt using continuous reactive extrusion described in detail elsewhere.[15] This ethylene/1-octene copolymer (ENGAGE^{TM}8407) has 7.3–7.7 mol % octene with a MFR of 30 dg/min and density of 0.870 g/cm^3. The MFR of PE-MA was ~5 g/10 min, and the anhydride content was determined to be 0.75 wt % by a calibrated FTIR analytical method. A total of 0.75 wt % corresponds to about one succinic anhydride group per 1000 —CH_2— units on the polyolefin backbone. The hydroxy- and amino-functional analogs were then prepared directly from PE-MA by reactive extrusion with 2-aminoethanol and *N*-methyl-1,3-propanediamine as described by Silvis et al.[15] The relative concentrations of OH and NHR functionalities, *N*-(2-hydroxyethyl)-succinimide and *N*-(3-(*N*-methylamino)-1-propyl)-succinimide were 1.08 wt % and 1.28 wt %, respectively, based on complete conversion of the anhydride to functionalized imide as determined using FTIR spectroscopy (anhydride C=O at 1790 cm^{-1}; imide C=O at 1705 cm^{-1}). Because of crosslinking side reactions, the MFR dropped to ~5 g/10 min after grafting with MA; however, the density and octene content were essentially unchanged. Conversion of MA to OH or NHR did not alter the MFR any further. The structures of LLDPE-1 and functional PEs are given in Figure 1.

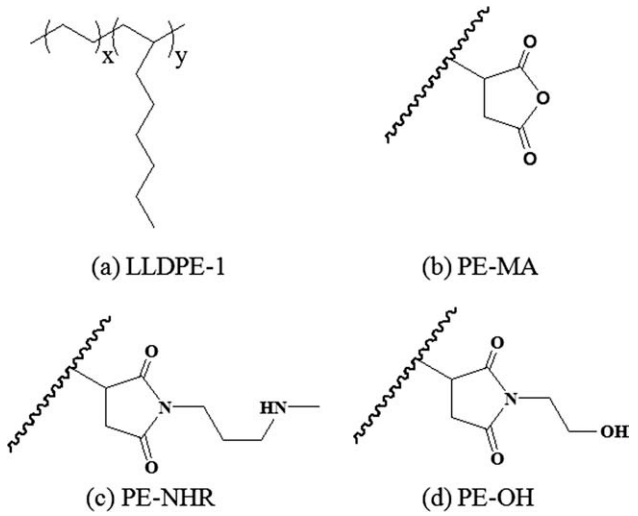

Figure 1. Structures of the functional polyethylenes used in this study.

a: LLDPE-1 (ethene/1-octene random copolymer; $x/y = 93/7$); (b): Succinimide *grafted* polyethylene (PE-MA); (c):*N*-(3-(*N*-methylamino)-1-propyl)-succinimide *grafted* polyethylene (PE-NHR); (d): *N*-(2-hydroxyethyl)-succinimide *grafted* polyethylene (PE-OH). Wiggly chains in (b), (c), (d) represent ethene/1-octene random copolymer backbones.

TPU (Avalon® 70 AE) with polyester soft segments was provided by Huntsman Polyurethanes. It has a number average molecular weight of 77.5 kg/mol and PDI 1.7 based on polystyrene standards (EasiCal PS-2, Polymer Laboratories) as determined by size exclusion chromatography (SEC, Waters 717 Plus HPLC Autosampler) at room temperature using tetrahydrofuran (THF) as a mobile phase. Key properties of PEs and TPU are listed in Table 1.

TPU pellets were dried overnight in a conventional static oven at ~70°C to remove residual moisture before

Table 1. Key Properties of PEs and TPU

	LLDPE-1	PE-MA	PE-OH	PE-NHR	TPU
T_m (°C)	67	66	67	67	152
Crystallinity (%)	9.4	8.3	8.8	8.5	–
Density (g/cm^3)	0.87	0.87	0.87	0.87	1.21
Viscosity[a] (Pa·s)	6.3×10^2	–	–	–	8.8×10^2

[a]Dynamic viscosity at frequency equal to the apparent wall shear rate at the die exit, 63 s^{-1}.

compression molding and coextrusion. The viscosities were measured at 180°C under N_2 atmosphere by a strain controlled rotational rheometer (ARES, TA Instruments) using 25 mm parallel plates. Differential scanning calorimetry (DSC) measurements were performed with TA Instruments DSC Q1000. Approximately 10 mg of dry polymers were loaded into non-hermetic aluminum pans. DSC scans were performed at the rate of 10°C/min from −100 to 250°C. Melting temperature was determined from the first scanning cycle using TA Instruments Universal Analysis 2000 software.

Dynamic viscosity and storage modulus values at 180 °C for TPU and all the functional PE/LLDPE-1 blends were similar, within ±10%, over the frequency range 10–100 rad/s. Matching viscosity and elasticity is important to prevent layer nonuniformities or even instability.[16] A less viscous polymer may encapsulate a more viscous polymer as they flow through a channel. Elastic polymers flow through a rectangular die can give rise to rearrangement of layer thicknesses. The coextrusion line was allowed to run for at least half an hour before sample collection to achieve steady state. No interfacial instability was observed.

The maximum shear rate at the die wall was 63 s^{-1}. By using the dynamic viscosity of the polymer melt at this shear rate, the shear stress at the wall was calculated to be 10.7 Kpa. In the feedblock, the maximum shear rate at the wall was 101.1 s^{-1} and shear stress 12.2 Kpa.

Melt blending

LLDPE-1 and functional PEs were blended with a 16 mm co-rotating twin-screw extruder (Prism Engineering, Staffordshire, England) at 100 rpm. This extruder has a length-to-diameter ratio of 25 and five temperature control zones and a mixing screw configuration with three kneading elements and one backflow element.[17] The barrel temperatures from hopper to die exit were set at 100, 130, 165, 180, and 180°C. The extruded functional PE/LLDPE-1 strand was cooled in an ice water bath and pelletized. All samples were dried at ambient condition for at least 1 week before use.

Lamination and T*-peel test*

Functional PE/LLDPE-1 and TPU films (80 mm × 7.5 mm × 0.4 mm) were prepared by compression molding from pellets at 120°C and 180°C, respectively, under 2 MPa between two polytetrafluoroethylene-(PTFE) coated aluminum foils (Saint-Gobain Performance Plastics). Functional PE/LLDPE-1 and TPU films were dried in vacuum oven at room temperature and 70°C, respectively. After drying under vacuum, TPU and functional PE/LLDPE-1 films were pressed into intimate contact sandwiched within two PTFE-coated aluminum foils and annealed for various time at 180°C under 0.1 MPa within a rectangular mold (80 mm × 7.5 mm × 0.75 mm).

Immediately after annealing, bilayer samples were quenched by plunging into ice water. The edges of bilayer samples were trimmed with a razor blade, and *T*-peel tests were conducted 24 h after lamination. A MINIMAT tensile tester (Rheometric Scientific) with an extension rate of 1 mm/s was used to peel the bilayer. Peel strength was defined as the ratio of the median plateau value of peeling force (F) over peeling arm width (b). At least three samples were tested for each experimental measurement, and the mean values as well as the standard deviations were calculated. To generate more flow during melt lamination, a pair of thicker layers (0.6 mm instead of 0.4 mm) were squeezed down to 0.75 mm.

Coextrusion

The functional PE/LLDPE-1 and TPU bilayer samples were prepared by coextrusion at 180°C through dies shown schematically in Figure 2. TPU was delivered by a single-screw extruder to a gear pump (Zenith PEP-II), which controlled the flow rate to the feedblock. Compounded functional PE/LLDPE-1 pellets were fed by the 16 mm twin-screw extruder. Functional PE/LLDPE-1 and TPU were extruded at equal flow rate. A detailed description of the coextrusion line can be found in the literature.[8,18–20] Based on the continuity equation, melt velocity in the coextrusion dies can be deduced from the chill roll speed and film thickness. At a total flow rate of 38.4 cm^3/min as determined from calibrated gear pumps, the average linear velocity of the polymer melt in the die land was about 10 mm/s. Thus, the residence time in the sheeting die and die land was less than 10 s. Upon exiting the die land, bilayer films were drawn by chill rolls at 4°C. The temperature of molten polymer was measured by an infrared thermometer (Omega Engineering, Inc.). The die exit has dimension of 50 mm × 1.2 mm. The thickness of bilayer samples varied from 0.4 mm to 1 mm depending on take-up velocities of the chill rolls. *T*-peel tests on coextruded films were conducted by using the same procedure as described in the previous section.

Results and Discussion

Lamination

A typical plot of peel strength vs. crosshead displacement is shown in Figure 3. During a *T*-peel test, one end of a bilayer specimen is fixed, whereas the other end is pulled away at 180° by a moving grip at a constant velocity. Peel strength was determined by taking the average of all F/b values starting from the onset of peeling. In Figure 4, adhesion strength, F/b, is plotted vs. functional group type, functional PE content and annealing time for laminated bilayers.

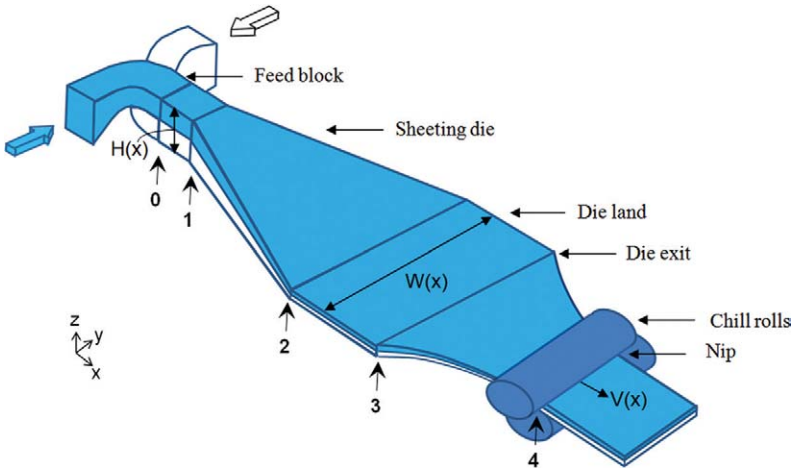

Figure 2. Schematic of polymer melt flowing through the coextrusion die followed by draw down from the die exit by the chill rolls.

[Color figure can be viewed in the online issue, which is available at wileyonlinelibrary.com.]

Lu et al.[12] have shown that at high temperature the urethane linkage in TPU dissociates to generate isocyanate, which can react with various functional groups. As a result, polyurethane and functional polyolefins can form copolymers from melt reaction. In this research, because the functional groups are randomly distributed along the backbones of the functional PEs, the coupling reaction between TPU and functional PEs are expected to form graft copolymers that bridge across the interface and improve adhesion. To better understand adhesion properties of functional PEs, the reaction rate between chain coupling is expressed in terms of Σ, the number of copolymer chains per interfacial area:

$$\Sigma = vt \tag{1}$$

where v is the effective two-dimensional coupling reaction rate in the interface (chains/s/m^2), t is reaction time (s). Σ can be evaluated from a T-peel test.

In a T-peel test, G_a, the fracture energy per unit crack propagation length, can be calculated by using the following energy analysis[21,22]:

$$G_a = \frac{F}{b}(1+\varepsilon_a - \cos\theta) - h\int_0^{\varepsilon_a} \sigma d\varepsilon - G_{db} \tag{2a}$$

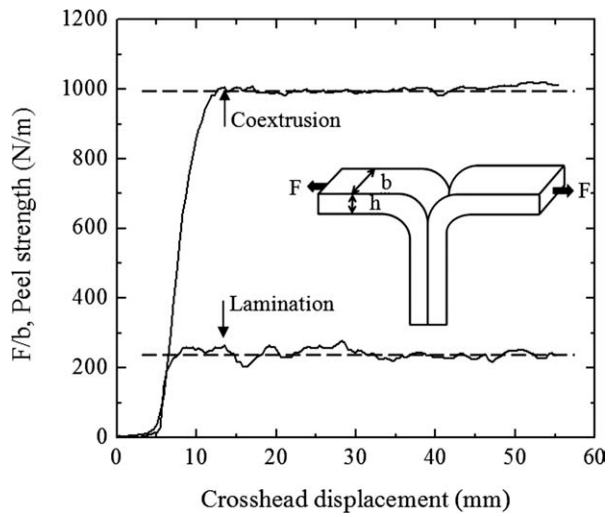

Figure 3. Peel strength, *F/b*, vs. crosshead displacement for *T*-peel tests of 3 wt % PE-NHR /TPU bilayers.

Dashed line represents the median plateau values of bilayers with 30 s reaction time for lamination and residence time of 10 s for coextrusion. A schematic drawing of the T-peel test is also shown where b and h denote the peel arm width and thickness respectively, and F is the peeling force.

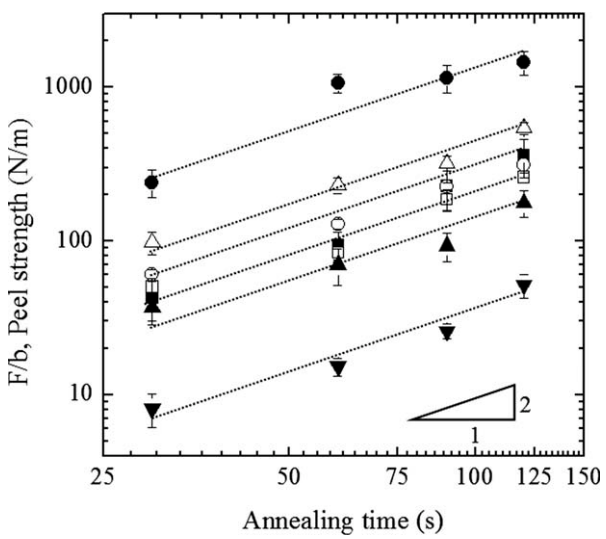

Figure 4. Peel strength, *F/b*, of laminated bilayers vs. content of incorporated functional PE and annealing time.

■, ●: 1 and 3 wt % PE-NHR; ▼, ▲: 3 and 10 wt % PE-OH; □, ○, △: 10, 20, and 30 wt % PE-MA. Error bars represent standard deviation of three to six tests. The solid lines are used to guide the eye.

where F is peeling force, b is the peeling arm width, h is the peeling arm thickness, ε_a is strain in the peeling arms, θ is peeling angle (90° for T-peel test), σ is the stress at the cross-section of the peeling arm, and G_{db} is bending energy. G_{db} is negligible for the thin flexible films made from the low modulus elastomers used in this research. When there is negligible change on peeling arm width, $\frac{F}{b}\varepsilon_a \approx h\int_0^{\varepsilon_a}\sigma d\varepsilon$. Based on this analysis, Eq. 2(a) simplifies to $G_a = F/b$. G_a can be related to G_c, the critical energy release rate,[23] which is the intrinsic material toughness, by

$$G_a = G_c(1 + \Phi(\dot{\varepsilon}, T)) \tag{2b}$$

where Φ is a function of peeling rate $\dot{\varepsilon}$, and temperature T. Combining Eqs. 2(a) and 2(b) gives

$$\frac{F}{b} = G_c(1 + \Phi(\dot{\varepsilon}, T)). \tag{3}$$

Thus, when T-peel tests are conducted at constant peeling rate $\dot{\varepsilon}$ and temperature T, F/b is proportional to G_c.

In Figure 4 for the same type of functional PE, peel strength, F/b, increased with the amount of functional PE and annealing time. Log peel strength (F/b) vs. log annealing time has a slope of ~2. As by Eq. 1 areal density of chains, Σ, is proportional to reaction time, t, then F/b is proportional to Σ^2. Then applying Eq. 3 gives G_c proportional to Σ^2. G_c is a linear function of Σ if the interface failure occurs by simple chain scission or chain pull-out without any extensive plastic deformation, while it scales with Σ^2 if the applied interfacial stress is sufficient to activate plastic deformation of a small volume at the crack tip.[7,24] For elastomers, G_c includes the energy to break the intrinsic interfacial bonding and also the energy dissipated locally ahead of the peel front at the crack tip.[22] Clearly, the grafted copolymers generated via coupling between TPU and functional PEs were able to entangle across their interfaces and provide high adhesion strength. When peel strength F/b exceeded 500 N/m, plastic deformation of peeling arms was observed. Although there is no simple relationship correlating peel strength F/b and critical energy release rate G_c when there is significant plastic deformation,[25,26] it is the increase of chain density Σ that leads to increased peel strength.

To understand the effect of reactive species concentration on interfacial coupling reaction rate, we varied the concentration of functional PEs. The two-dimensional reaction rate in the interface, v, as defined in Eq. 1, can be determined as follows:

$$v = kC_X^a\lambda \tag{4}$$

where k is the usual three-dimensional reaction rate coefficient, C_X is the concentration of functional groups at the interface, a is the reaction order, and λ is the interfacial thickness (the effective distance over which the reactive groups can interact). The bulk concentration of urethane groups is at least 100 times higher than that of grafted functional groups on functional PEs, and therefore, urethane concentration can be considered constant. C_X is the concentration of functional groups on the PEs. $F/b \sim \Sigma^2$ gives $F/b \sim v^2$ such that we correlate peel strength with reaction rate. We found that the reaction order, a, was 0.95 for NHR, close to first order which might be expected for bimolecular collisions with a large excess of one reactant. However a decreased to 0.78 for OH and 0.45 for MA. These lower reaction orders may be due to the fact that the initial concentration of reactive species is higher in OH and MA grafted PE blends in contrast to NHR. This could lead to a more crowded interface reducing the effective concentration of functional groups.[27]

The reaction rate can be extracted from adhesion data by combining Eq. 1 and

$$\Sigma = \frac{\lambda\alpha\rho\varphi N_{AV}}{M_n} \tag{5}$$

where λ, α, ρ, φ and M_n are the interface thickness, conversion, density, concentration of functional PE in the blend, and the number-average molecular weight of functional PE. Assuming λ equals to 1–5 nm and conversion α is 1–5% at 120 s for PE-NHR, then Σ is 0.0006−0.006 chains/nm^2. By combining with Eq. 1, the reaction rate coefficient k in Eq. 4 has a range of 10^{-4}–10^{-3} s^{-1}.

This result can be compared to homogeneous reaction rate data obtained by Lu et al.[12] on small molecules in dimethyl sulfoxide (DMSO). The reaction between dioctyl 4,4′-methylenebis(phenyl carbamate) and octylamine follows second-order kinetics with an activation energy of 115 kJ/mol. Their data predicts a reaction rate constant of 5×10^{-4} L · mol^{-1} · s^{-1} at 180°C. By multiplying with urethane concentration, the apparent first order reaction rate coefficient is $k \sim 10^{-6}$ s^{-1}. The rate coefficient for urethane and secondary amine will be predicted to be even smaller than this. Therefore, the reaction rate between two immiscible reactive polymers in a molten interface was significantly higher than that of small molecule analogues in solution. Zhang et al.[8] and Feng and Hu[28] also observed similar phenomena. This is not surprising considering increased collision probability originating from longer relaxation time of reactive polymer chains holding functional groups at the interface.

Almost no adhesion was found between PE and TPU. Among different functional PEs, moderate improvement was achieved by adding MA and OH modified PEs. Surprisingly, peel strength with only 3 wt % PE-NHR increased dramatically to $F/b \sim 1000$ N/m within only 60 s annealing time, indicating a fast reaction between urethane linkages and secondary amine groups.

Coextrusion

Figure 5 shows that for coextruded bilayer samples, peel strength decreased with drawdown ratio, the ratio of velocity of polymer at the nip point of chill rolls over velocity of polymer at the die exit. The interfacial copolymer density, Σ, is calculated to understand the effect of drawdown on adhesion.

To calculate Σ, the region where reaction occurred must be determined. Figure 2 shows that the two molten streams started contacting each other upon exiting the feed block. Copolymers were generated at the interface while the polymer streams flowed in the coextrusion die. Upon exiting the die, the temperature of the molten polymer decreased very little <5°C, until it touched the nip point, due to the low thermal diffusivity of polymers and relatively high film velocity.[29] Thus, the time polymer spends between the die exit

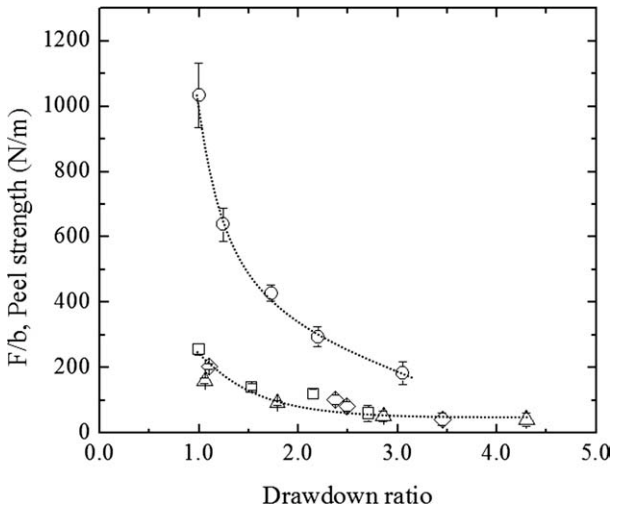

Figure 5. Peel strength vs. drawdown ratio for adhesion achieved by coextrusion at total volumetric flow rate $Q = 38.4$ cm^3/min.

□, ○: 1 and 3 wt % PE-NHR, △: 10 wt % PE-OH, ◇:20 wt % PE-MA. The solid line is used to guide the eye.

and the nip was taken into account as part of the reaction time calculation. To check whether chill rolls are effective enough to quench interfacial reaction by reducing temperature, we solved the unsteady state energy balance.[30] By assuming an isothermal boundary at 4°C, the time for the interface to be cooled below 60°C (~100°C lower than urethane dissociation temperature) is less than 0.5 s. We also observed that the temperature of coextrudate decreased to below 50°C after it passed through chill rolls, indicating that the interfacial reaction was terminated. Thus, the interfacial reaction in a coextrusion line begins in the region where polymer streams start contacting and ends at the chill roll nip.

The copolymer number density Σ is affected by both the residence time and the change of interfacial area during coextrusion. In the absence of reaction, an increase in the interfacial area (dilation) would dilute the areal density Σ. We consider this aspect when calculating the resulting copolymer number density via coextrusion. The calculation in the appendix gives the following conservation expression, which is a balance between creation and advection,

$$v = V_x \frac{\partial \Sigma}{\partial x} + V_y \frac{\partial \Sigma}{\partial y} + \left(\frac{\partial V_x}{\partial x} + \frac{\partial V_y}{\partial y} \right) \Sigma. \tag{6}$$

Here v is the effective two-dimensional reaction rate defined in Eq. 1, and V_x and V_y are the velocity at the interface in the flow- and spanwise-direction, respectively. The first two terms on the right hand side represent standard advection. The term in parentheses represents the dilation of the interfacial area due to stretching and cannot be neglected for this two-dimensional case (although in three-dimensions this term would equal zero for incompressible materials). Equation 6 is solved under the simplifying assumption of plug flow through the coextrusion die (i.e. perfect slip at the bounding wall), and the boundary condition $\Sigma\ (x = 0) = 0$:

$$\frac{\Sigma(x)}{v} = \frac{1}{Q} e^{\int_0^x f(x)dx} \left\{ \int_0^x e^{-\int_0^x f(x)dx} H(x) W(x) dx \right\} \tag{7}$$

where v has been factored out because it is an unknown constant, Q is the total volumetric flow rate through the die, $H(x)$ is the bilayer thickness in the z-direction, and $W(x)$ is the spanwise width in the y-direction. The term $f(x)$ is the area dilation term

$$f(x) = \frac{1}{H(x)} \frac{dH}{dx}. \tag{8}$$

The ratio Σ/v represents the effective reaction time during the coextrusion process, which is a combination of the residence time and any interfacial area dilation which occurs. We use the definition of effective reaction time,

$$t_{\text{eff}} \equiv \frac{\Sigma}{v} \tag{9}$$

as calculated via Eq. 7, to show the effect of drawdown on adhesion and to compare coextrusion and lamination experiments.

Figure 6 shows the solution of Eq. 7 for our coextrusion die for the draw down ratios used in Figure 5 for the PE-NHR samples. In section 0→1 and 2→3, because bilayer thickness $H(x)$ and spanwise width $W(x)$ do not change with x, Σ/v simplifies to $\Sigma/v = HW_x/Q$. Therefore, Σ/v is only a function of residence time and it increases linearly with position. In section 1→2 and 3→4, Σ/v is affected by both the residence time and the interfacial area dilation. The interfacial area dilation is caused by the change of die dimension in section 1→2 and drawdown in section 3→4. In section 3→4, increasing drawdown ratio gives rise to reduced t_{eff}. This is due to the fact that faster drawdown not only leads

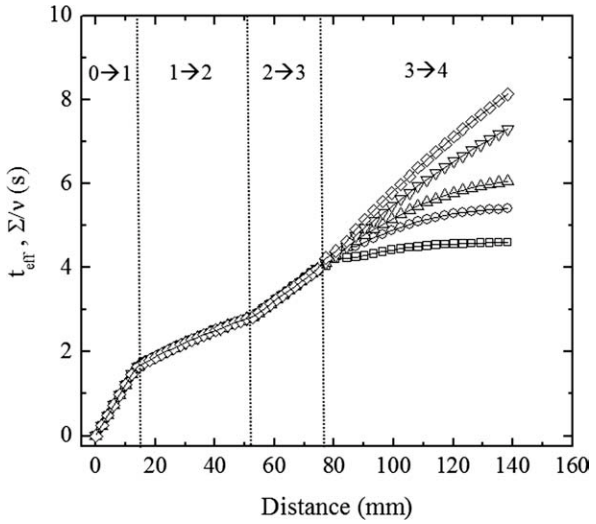

Figure 6. An illustrative solution for Eq. 7, t_{eff} vs. distance for different drawdown ratios taken from Figure 5 for 3 wt % PE-NHR.

The drawdown ratio values are as following ◇: 1.02, ▽: 1.24, △: 1.73, ○: 2.19, □: 3.05. Section 0→1, 1→2, 2→3, and 3→4 correspond to the notation in Figure 2.

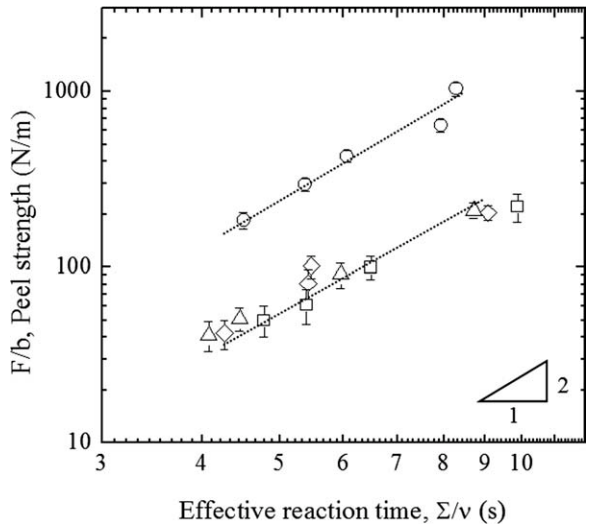

Figure 7. Peel strength data from Figure 5 plotted vs. effective reaction time, Σ/*v* for adhesion achieved by coextrusion.

□, ○: 1 and 3 wt % PE-NHR, △: 10 wt % PE-OH, ◇: 20 wt % PE-MA. The solid lines are used to guide the eye.

to shorter reaction time but also increased interfacial area. Both lead to reduced interfacial copolymer density, thus weaker adhesion.

The coextrusion peel strength values in Figure 5 were plotted vs. effective reaction time, Σ/*v* in Figure 7. As we expect from the results in Figure 6 increasing drawdown ratio leads to shorter effective reaction time and hence decreased peel strength. A similar phenomenon was observed by Morris,[31] where the peel strength between coextruded HDPE/Adhesive/EVOH films increased with process time.

For the same functional PE, all the data follow a double-log slope of 2, which agrees with the fundamental correlation[7] $G_c \propto \Sigma^2$. It is also shown in Figure 7 that 1 wt % PE-NHR, 10 wt % PE-OH, and 20 wt % PE-MA had similar reactivities while 3 wt % PE-NHR was much faster. This ranking agrees with the trend of lamination results in Figure 4. Consequently, lamination tests can be used to rank the adhesion strength expected for coextrusion of the same polymers.

Reaction acceleration through coextrusion

For lamination, the annealing time in Figure 4 was considered to be effective reaction time, because it takes less than 0.5 s for the bilayer interface to reach the command temperature (the heat transfer calculation for lamination is analogous to that for the chill rolls during coextrusion). For coextrusion, $t_{\text{eff}} = \Sigma/v$ was calculated according to Eq. 7. Thus, peel strength vs. effective reaction time for both lamination and coextrusion are compared in Figures 8a, b for different functional groups. Figure 8a shows that after 90 s of reaction for lamination, the interface of PE and TPU approached saturation with interfacial copolymers, i.e. peel strength approached a plateau value. Although for coextrusion, it took only about 8 s to reach the same value (i.e., about one order of magnitude faster than lamination).

It is apparent that the interfacial coupling reaction was greatly accelerated by coextrusion in comparison with lamination. As shown in Figures 8a, b, coextrusion accelerates the coupling reaction for all types of functional PEs. Similar phenomena were found in the literature where the coupling reaction between an amine-terminal polystyrene (PS-NH_2) and an anhydride-terminal polymethyl methacrylate (PMMA-anh) bilayer took about 1 h for the interface to be saturated with block copolymers, whereas when these two polymers were melt blended[11,28] or multilayer coextruded,[8] it took less than 1 min (i.e., about two orders of magnitude faster compared to quiescent annealing).

For the coextrusion experiments reported here, the reaction acceleration occurs during laminar flow without mixing. Furthermore, the interface is located in the middle of the die, where shear stress approaches zero. However, the interfacial plane does experience compression and extension during coextrusion, as do the bulk phases above and below the interface. As the molten polymer stream was converted from

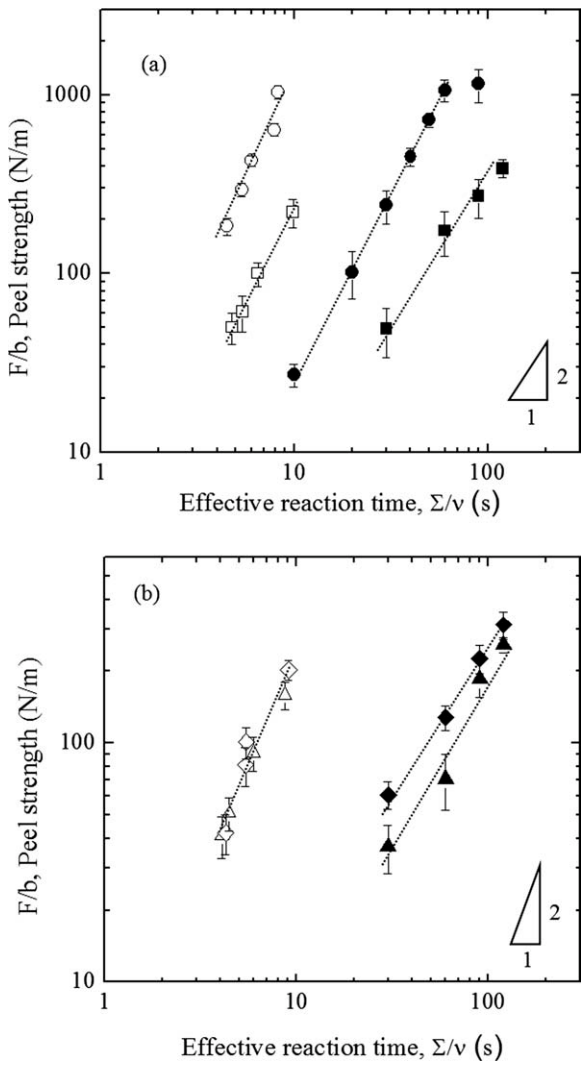

Figure 8. Peel strength comparison between lamination and coextrusion.

(a) 3 wt % PE-NHR: ○ (coextrusion), ●(lamination); 1 wt % PE-NHR: □ (coextrusion), ■ (lamination); (b) 20 wt % PE-MA: ◇ (coextrusion), ◆ (lamination); 10 wt % PE-OH: △ (coextrusion), ▲(lamination).

a square shape (10 mm × 10 mm) into a rectangular shape (1.2 mm × 50 mm) at the end of the fish-tail sheeting die, the interface of the bilayer experienced extensional strain (Hencky strain[32] $\varepsilon_{Henky} = 0.95$) in the machine direction (x), extensional strain ($\varepsilon_{Henky} = 1.4$) in the transverse direction (y), and compressive strain ($\varepsilon_{Henky} = 2.3$) in the z direction. Moreover, during draw down from the die exit to the nip, additional extension and compression were applied.

Under these compression/extension conditions, in the absence of shear or mixing, there are several possible causes of the increase of the interfacial reaction rate or the increase of the measured peel strength. These include induced crystallinity, enhanced diffusive flux of functional groups via compression of diffusion boundary layers, and increased concentration of functional groups in the interfacial region due to extensional and compressive flow in coextrusion. We will argue against crystallinity and show that enhanced diffusion alone cannot account for the dramatic increase in reaction rate. We, therefore, speculate that extensional and compressive flow in the coextrusion process contributes to the accelerated reaction rate during coextrusion.

Crystallinity is known to affect interfacial adhesion,[33,34] and this could increase the adhesive force even with constant copolymer reaction rate. We compared the crystallinity of laminated and coextruded functional PE/ LLDPE-1 blends and found that crystallinity was affected little by processing: 8–9% (pellets) and ~11% (coextrusion). The stress–strain curves were also the same for films produced by both lamination and coextrusion. Thus, crystallinity plays a negligible role in the observed increase in peel strength, and we must consider possible mechanisms for increasing the copolymer reaction rate.

We consider the general possibility of modifying diffusive flux or the local reaction process due to compressive flow normal to the interface. The absolute reaction rate is determined by the reaction-diffusion balance,

$$v = -D\frac{dC}{dz} \approx \frac{D(C_\infty - C_X)}{\delta} \tag{10}$$

where v is the two-dimensional coupling reaction rate in the interface, D is the diffusivity of the functional PE, C_∞ the volumetric density of grafted functional groups in the bulk, C_X is the volumetric density of grafted functional groups at the interface, and δ is the diffusion lengthscale. Assuming $a = 1$ for bimolecular collisions, combining Eqs. 4 and 10 gives

$$v = \frac{DC_\infty}{\delta + \frac{D}{k\lambda}}. \tag{11}$$

Equation 11 gives the reaction rate in terms of both diffusion and local reaction parameters. Flow of the bulk phase material to the interface will modify the concentration profile of the reactive species. Compressing the layered sample normal to the interfacial surface: (i) decreases the diffusion layer δ and (ii) may increase local reaction rate k by forcing polymer chains towards each other. Each mechanism will increase the reaction rate v as shown by Eq. 11. The relative importance of these two mechanisms is determined by the reaction being diffusion-limited or reaction-limited, i.e. the relative size of the terms in the denominator of Eq. 11. We compared reaction rate to transport rate by calculating Damköhler number in the Appendix and found that although decreasing the diffusion length scale δ due to external mass transfer will increase the reaction rate, such increase of diffusive flux would be negligible for the reaction-limited process studied here.

We are, therefore, left to conclude that reaction acceleration was mainly caused by an increase in the local reaction process and suggest that extensional and compressive flow in the coextrusion process gave rise to the reaction acceleration.

The interface between two immiscible polymers plays the role of an obstacle (or diffusion barrier) that hinders the diffusion of both reactive polymer chains to the interface for chemical reactions. Rafailovich[35] et al. found that the diffusion rate is one order of magnitude slower near an interface compared with in the bulk. We speculate that under coextrusion conditions, flow helps to force reactive species to penetrate into interface and increases the concentration of reactive species in the interface.

Macosko et al.[36] found that flow resulted in a rate constant over 1000 times higher in heterogeneous melt blending than that in the quiescent bilayer reaction for an amine-terminal polystyrene (PS-NH_2) and an anhydride-terminal polymethyl methacrylate (PMMA-anh) system. Although a significant amount of interface was generated during blending, the rate constant was still ~300 times higher than that of quiescent bilayer reaction after normalizing by interfacial area.[37] Apparently, the complex flow under mixing accelerated interfacial reaction.

Zhang et al.[8] found that for a similar system, the reaction rate in coextrusion is comparable to that achieved in heterogeneous blending, as well as in homogeneous melt reaction, where the same functional groups were attached to PS chains and brought together to react. Apparently flow in coextrusion also accelerated interfacial coupling reaction compared to quiescent bilayer reaction without the presence of flow. Moreover, flow may help to stretch the polymer chains and expose the functional groups thus increasing the probability of reactive groups colliding with each other.

In this study, the reaction rate difference between coextrusion and lamination is less than that measured for the primary amine/anhydride functional polymers.[8] In the PS/ PMMA system, functional groups tend to be depleted from the interface due to their high surface energy compared with that of the polymer backbones, leading to very slow coupling under quiescent conditions. However, the polar TPU backbones may attract the polar functional groups into the interface, leading to faster reaction. Additionally, the model study by lamination is different from quiescent reaction as some compressive flow is almost inevitable in lamination and flow accelerates interfacial reaction. Moreover, our functional groups are along the polymer chain, while Zhang et al.[8] observed the effect of extrusion acceleration of interfacial coupling with end functional chains and multilayer coextrusion.

It should be noted that for the drawdown process in coextrusion, we find that increased chill roll velocity gave increased reaction rate because of flow and decreased effective reaction time due to dilation of interfacial area. It seemed that the latter one was dominant with respect to the effect of drawdown. However, the overall coextrusion

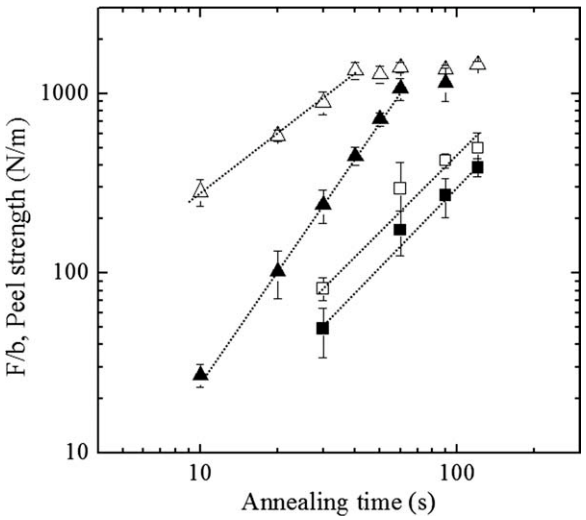

Figure 9. Peel strength comparison for lamination with different compressive strain.

3 wt % PE-NHR: △ ($\varepsilon_{Henky} = 0.47$), ▲ ($\varepsilon_{Henky} = 0.06$); 1 wt % PE-NHR: □ ($\varepsilon_{Henky} = 0.47$), ■ ($\varepsilon_{Henky} = 0.06$).

process still resulted in reaction acceleration compared with lamination at the same temperature and reaction time.

To test the hypothesis that compressive deformation normal to the interface accelerates interfacial reaction, we repeated some lamination tests with more flow as shown in Figure 9. For 3 wt % PE-NHR and TPU, a Hencky strain of 0.47 gave much higher peel strength than a Hencky strain of 0.06 at the same annealing time. Thus, when a larger compressive strain was applied normal to the interface, more copolymers were generated at the interface. This effect is less pronounced for 1 wt % PE-NHR, presumably due to the lower concentration of functional groups at the interface. Note in Figure 9 for the 3% samples, the difference between large strain and small strain compression decreases with annealing time. This is reasonable because there is no further flow during annealing after the initial compression.

Future studies can be designed to test the effect of compressive flow normal to the interface in contrast with compressive/extensional flow in the plane of the interface. This can be accomplished by modifying the current die design (Figure 2) to decouple these effects. Compressive flow normal to the interface can be generated by changing the height $H(x)$ while keeping width $W =$ constant, in contrast to compression/extension in the plane of the interface caused by varying the width $W(x)$ while keeping height $H =$ constant. Such tests would reveal the dependency of the reaction rate v on the strength of the compressive flow $\dot{\varepsilon}$, and these results would be a guide to developing a more specific molecular theory to explain the increase in reaction rate observed in this study.

Conclusions

Adhesion between PE and thermoplastic polyurethane was improved by blending functional PEs into nonmodified PE. Direct measurements of interfacial adhesion were obtained using a *T*-peel test. We investigated the influence of functional group type, annealing time, concentration of incorporated functional PEs, and processing methods on interfacial adhesion. We were able to convert the effects of all these variables on adhesion to interfacial copolymer coverage. The ranking of adhesion strength of functional PE with TPU was determined as follows: NHR $\gg$ OH $\sim$ MA for both lamination and coextrusion processes. Particularly, amine functional PE showed dramatic improvement in adhesion with quite small incorporated amount. This ranking of functional groups agrees with reaction rates measured on model urethanes.[12] We also found increased adhesion strength with annealing time and concentration of incorporated functional PEs, as these effects resulted in increased interfacial copolymer coverage. Based on the calculation of interfacial copolymer coverage, reaction rates for two processes, lamination and coextrusion, were compared. Interfacial coupling reaction was found to be accelerated as much as an order of magnitude through coextrusion in comparison with lamination. We also found that the interfacial coupling rate in lamination could be increased by increasing the amount of compressive flow. This result is attributed to an increased concentration of functional groups in the interfacial region that results from the extensional and compressive flow in the coextrusion process forcing reactive species to penetrate into interface. Comparison to literature reaction rate data for small molecule amines with urethane groups in solution indicate that interfacial reactions in polymer melts are substantially faster. Beyond its scientific significance, this work illustrates why coextusion is so successful for producing multilayer products within a very short residence time.

Acknowledgment

This research has been supported in part by The Dow Chemical Company and IPRIME (the Industrial Partnership for Research in Interfacial and Materials Engineering) at the University of Minnesota. The authors are grateful for helpful discussions with Timothy Lodge and Jianbin Zhang. Parts of this work were carried out in the University of Minnesota I.T. Characterization Facility, which receives partial support from NSF through the NNIN program.

Literature Cited

1. Boaen NK, Hillmyer MA. Post-polymerization functionalization of polyolefins *Chem Soc Rev*. 2005;34:267–275.
2. Liston EM, Martinu L, Wertheimer MR. Plasma surface modification of polymers for improved adhesion: a critical review. *J Adhes Sci Technol*. 1993;7:1091–1127.
3. Mori M, Uyama Y, Ikada Y. Surface modification of polyethylene fiber by graft polymerization. *J Polym Sci: Part A: Polym Chem*. 1994;32:1683–1690.
4. Goddard JM, Hotchkiss JH. Tailored functionalization of low-density polyethylene surfaces. *J Appl Polym Sci*. 2008;108:2940–2949.
5. Jia S, Xu D, Mai B, Zhang M, Rong M. Localized compatibilization in immiscible blends of thermoplastic polyurethane and ethylene-octylene copolymer. *J Appl Polym Sci*. 2007;105:1309–1315.
6. Creton C, Kramer EJ, Hui C-Y, Brown HR. Failure mechanisms of polymer interfaces reinforced with block copolymers. *Macromolecules*. 1992;25:3075–3088.
7. Boucher E, Folker JP, Creton C, Hervet H, Leger L. Enhanced adhesion between polypropylene and polyamide-6: role of interfacial nucleation of the β-crystalline form of polypropylene. *Macromolecules*. 1997;30:2102–2109.
8. Zhang J, Ji S, Song J, Lodge TP, Macosko CW. Flow accelerates interfacial coupling reactions. *Macromolecules*. 2010;43:7617–7624.

9. Sha Y, Hui CY. Fracture toughness and failure mechanisms of epoxy/rubber-modified polystyrene (HIPS) interfaces reinforced by grafted chains. *Macromolecules*. 1996;29:4728–4736.
10. Cole PJ, Cook RF, Macosko CW. Adhesion between immiscible polymers correlated with interfacial entanglements. *Macromolecules*. 2003;3:2808–2815.
11. Zhang J, Lodge TP, Macosko CW. Interfacial morphology development during PS/PMMA reactive coupling. *Macromolecules*. 2005;38:6586–6591.
12. Lu Q, Hoye TR, Macosko CW. Reactivity of common functional groups with urethanes: models for reactive compatibilization of thermoplastic polyurethane blends. *J Polym Sci: Part A Polym Chem*. 2002;40:2310–2328.
13. Lu Q, Macosko CW. Promoting adhesion to thermoplastic polyurethane (TPU) by amine functional polypropylenes. *Polym Mater Sci Eng*. 2003;89:844–847.
14. Lu Q, Macosko CW, Horrion J. Melt amination of polypropylenes. *J Polym Sci: Part A Polym Chem*. 2005;43:4217–4232.
15. Silvis CH, Hahn SF, Pawlowski DF, Ansems P, Mergenhagen LK, Lakrout H, Inventors. Functionalized olefin polymers, compositions and articles prepared therefrom, and methods for making the same. WO 0800812008, 2008.
16. Anderson PD, Dooley J, Meijer HEH. Viscoelastic effects in multilayer polymer extrusion. *Appl Rheol*. 2006;16:198–205.
17. Spitael P, Macosko CW. Strain hardening in polypropylenes and its role in extrusion foaming. *Polym Eng Sci*. 2004;44:2090–2100.
18. Zhao R, Macosko CW. Slip at polymer-polymer interfaces: rheological measurements on coextruded multilayers. *J Rheol*. 2002; 46:145–167.
19. Lee PC, Park HE, Morse DC, Macosko CW. Polymer-polymer interfacial slip in multilayered films. *J Rheol*. 2009;53:893–915.
20. Dolgovskij M. Dispersing layered silicates in polymer melts: Using melt rheology to determine dispersion. PhD Thesis, University of Minnesota, 2007.
21. Kinloch AJ, Lau CC, Williams JG. The peeling of flexible laminates. *Inter J Frac*. 1994;66:45–70.
22. Kinloch AJ. Adhesives in engineering. *Proc Instn Mech Eng*. 1997;211:307–335.
23. Georgiou I, Hadavinia H, Ivankovic A, Kinloch AJ, Tropsa V, Williams JG. Cohesive zone models and the plastically deforming peel test. *J Adhesion*. 2003;79:239–265.
24. Dai C, Kramer EJ, Washiyama J, Hui C. Fracture toughness of polymer interface reinforced with diblock copolymer: effect of homopolymer molecular weight. *Macromolecules*. 1996;29:7536–7543.
25. Wei Y, Hutchinson JW. Interface strength, work of adhesion and plasticity in the peel test. *Intl J Frac*. 1998;93:315–333.
26. Hadavinia H, Kawashita L, Kinloch AJ, Moore DR, Williams JG. A numerical analysis of the elastic-plastic peel test. *Eng Fract Mech*. 2006;73:2324–2335.
27. Fredrickson GH, Milner ST. Time-dependent reactive coupling at polymer-polymer interfaces. *Macromolecules*. 1996;29:7386–7390.
28. Feng L, Hu G. Reaction kinetics of multiphase polymer systems under flow. *AIChE J*. 2004;50:2604–2612.
29. Morris BA. Understanding why adhesion in extrusion coating decreases with diminishing coating thickness. *J Plast Film Sheet*. 2008;24:53–88.
30. Bird RB, Stewart WE, Lightfoot EN. *Transport Phenomena*. John Wiley, 2007.
31. Morris BA. The effect of processing variables on peel strength performance in coextrusion blown film. *SPE-ANTEC Tech Pap*. 1996;42:116–120.
32. Macosko CW. *Rheology-Principles, Measurements, and Applications*. New York: Wiley, 1994.
33. Seo Y, Ninh TH. Enhanced interfacial adhesion between polypropylene and nylon 6 by in situ reactive compatibilization. *Polymer*. 2004;45:8573–8581.
34. Seo Y, Kang T. Interfacial adhesion between semi-crystalline polymers (polypropylene and nylon-6): in situ compatibilized interface and fracture mechanism. *Compos Interface*. 2006;13:605–621.
35. Zheng X, Rafailovich MH, Sokolov J, Strzhemechny Y, Schwarz SA, Sauer BB, Rubinstein M. Long-range effects on polymer diffusion induced by a bounding interface. *Phys Rev Lett*. 1997;79:241–244.
36. Macosko CW, Jeon HK, Hoye TR. Reactions at polymer-polymer interfaces for blend compatibilization. *Prog Polym Sci*. 2005; 30:939–947.
37. Jeon HK, Macosko CW, Moon B, Hoye TR, Yin Z. Coupling reactions of end- vs mid-functional polymers. *Macromolecules*. 2004;37:2563–2671.
38. Bartels CR, Crist B, Graessley WW. Self-diffusion coefficient in melts of linear polymers: chain length and temperature dependence for hydrogenated polybutadiene. *Macromolecules*. 1984;17:2702–2708.
39. Panajotova BV, Herman MF. A quantitative theory of linear chain polymer dynamics in the melt. IV. Comparison with experimental diffusion constant data. *J Chem Phys*. 1998;108:5122–5129.
40. Oyama HT, Inoue T. Kinetics and mechanism of coupling of functionalized chains at the immiscible polymer-polymer interface. *Macromolecules*. 2001;34:3331–3338.
41. O'Shaughnessy B, Vavylonis D. Reactive polymer interfaces: how reaction kinetics depend on reactivity and density of chemical groups. *Macromolecules*. 1999;32:1785–1796.
42. Schulze JS, Cernohous JJ, Hirao A, Lodge TP, Macosko CW. Reaction kinetics of end-functionalized chains at a polystyrene/poly(methyl methacrylate) interface. *Macromolecules*. 2000; 33: 1191–1198.

Appendix

Copolymer mass conservation in the two-dimensional interface

Here, we derive the equations used to model the mass transport of copolymer compatibilizer chains created at the interfacial region during coextrusion. We assume that created copolymer chains remain at the interface but may diffuse or advect within the two-dimensional x-y plane at the interface. The mass conservation equation balances creation and transport, and in this two-dimensional plane it is given by

$$v = \nabla_{xy} \cdot (\mathbf{j}'). \tag{A1}$$

Here, v is the two-dimensional reaction rate (chains/s/m^2), ∇_{xy} is the gradient operator which operates only within the plane, $\nabla_{xy} \equiv d/dx + d/dy$, and $\mathbf{j}'$ is the rate of copolymer flux per unit length which occurs only within the x-y plane. The mass flux can be caused by advection or diffusion,

$$\mathbf{j}' = \mathbf{V}\Sigma - D\nabla_{xy}\,\Sigma \tag{A2}$$

where $\mathbf{V}$ is the velocity vector in the plane, $\mathbf{V} = (V_x, V_y)$, and D is the diffusivity. For our situation, we can show that diffusion is negligible compared to advection by the flow.

The relative importance of advection to diffusion is determined by the Peclet number, which we estimate to be large, $Pe = VL/D \approx 10^{13}$. This is estimated using a characteristic flow velocity $V \sim L/t$ with maximum contact time $t \sim 11.4$ s, process length $L \sim 14$ cm, and diffusivity $D \sim 10^{-12}$ cm^2/s.[38,39] Combining Eqs. A1 and A2 and neglecting diffusive flux gives the conservation expression,

$$v = V_x \frac{\partial \Sigma}{\partial x} + V_y \frac{\partial \Sigma}{\partial y} + \left(\frac{\partial V_x}{\partial x} + \frac{\partial V_y}{\partial y} \right) \Sigma \tag{A3}$$

which is a balance between creation and advection. Equation A3 is a first order partial differential equation with nonconstant coefficients for the areal number density Σ (x,y), which depends on the velocity field at the interface $\mathbf{V}$ (x,y) and the

reaction rate v. We will derive a solution to Eq. A3 under simplifying assumptions to calculate the number density Σ which results at the end of the coextrusion process.

For our estimate we assume plug flow (i.e., perfect slip at the bounding walls), for which the velocity in the flow direction is only a function of x, i.e., V_x (x) throughout the entire volume. Consistent with plug flow, we further assume that copolymer density is also only a function of x, therefore $d\Sigma/dy = 0$. With the plug flow assumption, we can relate the flow velocity V_x to the input flow rate Q by continuity,

$$V_x(x) = \frac{Q}{A(x)} \tag{A4}$$

where $A(x)$ is the local area. For our rectangular cross section $A(x) = H(x)W(x)$, where $H(x)$ is the bilayer thickness in the z-direction and $W(x)$ is the spanwise width in the y-direction. The parameters Q, $H(x)$, and $W(x)$ are known, and therefore, $V_x(x)$ and dV_x/dx can be calculated for use in Eq. A3. As our final required input to Eq. A3, we derive an expression for the stretching in the spanwise direction dV_y/dy. For plug flow, stretching in the y-direction is directly determined by the confinement in the y-direction $W(x)$. The interface length in the y-direction must always match $W(x)$, and is carried along by flow in the x-direction. Assuming a linear velocity profile of V_y (y), with V_y ($y = 0$) $= 0$, leads to the following expression

$$\frac{dV_y}{dy} = \frac{V_x}{W}\frac{dW}{dx} \tag{A5}$$

where each variable on the right hand side is a function of only x. Finally, we combine the plug flow velocity field results, Eqs. A4 and A5, with the conservation expression, Eq. A3, to yield a first order differential equation for the areal number density $\Sigma(x)$,

$$\frac{d\Sigma}{dx} - \frac{1}{H(x)}\frac{dH}{dx}\Sigma = \frac{v}{V_x(x)}. \tag{A6}$$

The coefficient in front of Σ results from dilation of interfacial area during coextrusion; this term equals zero when the interfacial area is kept constant, for which case the resulting number density $\Sigma(x)$ would be simply governed by the residence time $f_{res} = \int_0^x dx/V_x$. The full form of Eq. A6, including the possibility of interfacial area dilation, can be solved analytically. The result is Eq. 7 in the discussion section.

Damköhler number estimate

The Damköhler number, Da, effectively compares reaction rate to transport rate, defined here as

$$\mathrm{Da} = \frac{\text{Reaction rate}}{\text{Diffusion rate}} = \frac{kC_X\lambda}{DC_\infty/\delta}. \tag{A7}$$

The reaction is diffusion limited for $Da \gg 1$ and reaction-limited for $Da \ll 1$. We estimate the range of Damköhler number from the range of possible parameter values. The reaction constant k in Eq. A7 is determined to be 10^{-3}–10^{-4} s^{-1} from adhesion test. The reactive species are grafted onto polymer chains, and we, therefore, choose a diffusivity D which is representative of polymer–polymer diffusion, $D = 10^{-13} - 10^{-11}$ cm^2/s.[38,39] For the interfacial thickness, we consider the value $\lambda \approx 5$ nm. For the diffusion length, we consider that the transient concentration boundary layer grows as $\delta(t) \sim \sqrt{Dt}$. Finally, for processing time $t \approx 1 - 10$ s, and the range of diffusivity and $D = 10^{-13} - 10^{-11}$ cm^2/s, we calculate the range of diffusion lengthscale $\delta \approx 3 - 100$ nm. For the given ranges of parameter values, we calculate a minimum and maximum Damköhler number, with the result that $Da \sim 10^{-7} - 10^{-2}$. Even the upper-bound estimate $Da \sim 10^{-2}$ is very small, and we conclude that the process is reaction-rate limited. Reactive polymer interfaces have been shown to be reaction limited for several other systems as well.[40–42]

Manuscript received Sep. 2, 2010, and revision received Jan. 3, 2011.